

Climate Signal Detection Using Wavelet Transform: How to Make a Time Series Sing

K.-M. Lau and Hengyi Weng*
Laboratory for Atmospheres,
NASA/Goddard Space Flight Center,
Greenbelt, Maryland

Abstract

In this paper, the application of the wavelet transform (WT) to climate time series analyses is introduced. A tutorial description of the basic concept of WT, compared with similar concepts used in music, is also provided. Using an analogy between WT representation of a time series and a music score, the authors illustrate the importance of *local* versus *global* information in the time-frequency localization of climate signals. Examples of WT applied to climate data analysis are demonstrated using analytic signals as well as real climate time series. Results of WT applied to two climate time series—that is, a proxy paleoclimate time series with a 2.5-Myr deep-sea sediment record of $\delta^{18}\text{O}$ and a 140-yr monthly record of Northern Hemisphere surface temperature—are presented. The former shows the presence of a 40-kyr and a 100-kyr oscillation and an abrupt transition in the oscillation regime at 0.7 Myr before the present, consistent with previous studies. The latter possesses a myriad of oscillatory modes from interannual (2–5 yr), interdecadal (10–12 yr, 20–25 yr, and 40–60 yr), and century (~180 yr) scales at different periods of the data record. In spite of the large difference in timescales, common features in time-frequency characteristics of these two time series have been identified. These features suggest that the variations of the earth's climate are consistent with those exhibited by a nonlinear dynamical system under external forcings.

1. Introduction

Wavelet transform (WT) is an analysis tool well suited to the study of multiscale, nonstationary processes occurring over finite spatial and temporal domains. Since its introduction by Morlet (1983) over a decade ago, WT has found wide application in diverse fields of sciences, such as seismic signal detection, image processing, optics, turbulence, quantum me-

chanics, chaos, fractal and medical research, etc. While the earth climate system undoubtedly possesses the above-mentioned characteristics, it seems somewhat befuddling that there is still a dearth of usage of WT in research on climate signal detection and analysis. This apparent lack of interest by the climate community may be because most papers on WT tend to employ a mathematical language with which the average climate analyst is not always familiar. This gives rise to the paradigm that WT is merely a sophisticated procedure used by mathematics specialists for pure academic pursuit and therefore has limited practical application in climate research. Recently, wavelet analyses are beginning to make inroads into the traditional atmospheric and oceanographic literature (e.g., Gambis 1992; Kumar and Foufoula-Georgiou 1993; Gamage and Blumen 1993; Gao and Li 1993; Collineau and Brunet 1993; Meyers et al. 1993; Weng and Lau 1994; Gollmer et al. 1995). However, given the appeal of WT for the study of nonstationary geophysical processes, there is little doubt that WT is underused and underexplored for climate research. The motivation of this paper is to remedy this situation and to call attention to the usefulness of WT as a powerful tool for climate research that can provide new understanding of the earth's climate.

In this paper, we first introduce features of WT using analytic forms of signals commonly encountered in climate data analysis. Then we present results of WT on two well-known climate time series to demonstrate new insights that can be gained from WT. This paper also serves as a tutorial on WT for the nonspecialists by providing an analog of WT with music.

*Current affiliation: General Sciences Corporation (a subsidiary of Science Applications International Corporation), Laurel, Maryland.
Corresponding author address: Dr. K.-M. Lau, Code 913, NASA/GSFC, Greenbelt, MD 20771.

In final form 30 May 1995.

©1995 American Meteorological Society

2. Preliminaries

This section is intended as an introduction of WT to the novice. Readers who are familiar with the WT

concept can skip to the next section. We will not provide rigorous mathematical derivation here. For such, the readers are referred to many excellent review papers and textbooks in the literature (e.g., Morlet 1983; Combes et al. 1989; Chui 1992; Daubechies 1992; Ruskai et al. 1992; and many others).

a. Local and global concepts

In general, a climate signal represents the culmination of interactions among physical processes operating on a wide range of spatial and temporal scales. The range of processes involved extend over spatial scales of a few meters to thousands of kilometers and over timescales from hours to millions of years. As a first step in the detection of a climate signal, the climate parameter in question is often averaged over a large spatial domain, such as over the entire globe, the hemispheres, entire continents, or the oceans. While the spatial averaging eliminates some of the high-frequency fluctuations, the resulting averaged time series can still possess a wide range of variability in the time domain. More often than not a climate time series is nonstationary, consisting of a variety of frequency regimes that may be localized in time (relative to the entire time history) or may span a large portion of the data record. The occurrence of a climate event is represented, in part, by a set of *local* parameters characterizing its frequency, intensity, time position, and duration. The time-integrated characteristics of these localized signals provide the *global* information, which describes the temporal mean states over some averaging period. Often, two completely different time series with different local information may result in very similar mean states. Hence, it is important to recognize that it is the totality of both the *local* and the *global* information that constitutes a true climate signal.

An illustration of the *local* versus *global* concepts can be found in music. A piece of melody (a time series) may be written in a musical score (a representation of the time series in a 2D time–frequency domain). Each musical note represents a musical tone (a signal) that is characterized by four parameters: frequency (indicated by a vertical location), time position (indicated by a horizontal location), time duration (indicated by the *tempo*, and different notes¹), and intensity (indicated by *f*'s and *p*'s, as well as by *accent* and *crescendo/decrescendo*). It is obvious that if all the local information is omitted, there is

very little left in a piece of music. For example, if we count the occurrence of each tone in a piece of music, scaled by the same note unit, we will find the dominant tones being the elements of the main chord that belongs to either a *major* scale or a *minor* scale. This is the *global* information of a melody that is usually given at the beginning of the musical score, such as C major or A minor, etc. However, this global information says very little about the real content of the music, and many different kinds of music may share the same global information (say, with a C major). In fact, this global information corresponds to the dominant peaks in the power spectrum of a climate time series. Thus, we can see a strong parallel here between music and climate signal analysis. Clearly, to define a true climate signal, both local and global information need to be preserved. However, because of the uncertainty principle, it is impossible to achieve increasing frequency resolution without suffering reduced precision in time localization, and vice versa. Traditional analysis tools such as Fourier transform or time filters do not provide much flexibility in the choice of an optimal combination in the simultaneous representation of both local and global signals. As we shall show in the following, the WT is a tool that is ideally suited for such a purpose.

b. From Fourier to wavelet transform

In some way, WT is a generalized form of Fourier transform (FT) and windowed FT (WFT) (Gabor 1946). The Fourier transform uses sine and cosine base functions that have infinite span and are globally uniform in time. For a stationary time series with a pure sine-wave signal, its FT is a line spectrum (Fig. 1, left panel). The Fourier transform does not contain any time dependence of the signal and therefore cannot provide any *local* information regarding the time evolution of its spectral characteristics. The representation of a localized signal in FT is very inefficient and requires a large number of Fourier components. In an extreme case where a signal is represented by a delta function in time, the signal would be represented by an infinite number of components in FT representation. Moreover, if the time series is reversed in time, the new time series will have exactly the same FT representation, even though the local information of the two time series is completely different.

In a WFT, a time series is examined under a fixed time–frequency window with constant intervals in the time and frequency domains. When a wide range of frequencies is involved, the fixed time window of the WFT tends to contain a large number of high-frequency cycles and a few low-frequency cycles or parts of cycles (see Fig. 1, middle panel). This often results in an overrepresentation of high-frequency

¹The musical notes represent different time length at dyadic scale: the whole note, half note, quarter note, eighth note, etc.

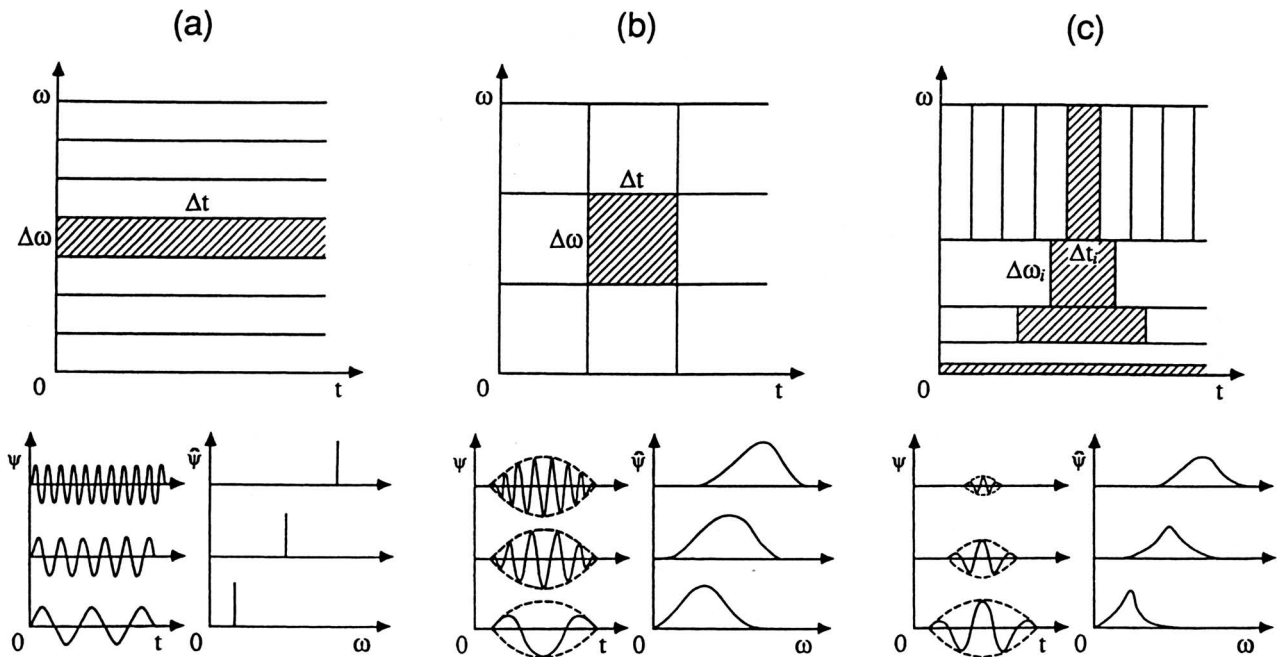


Fig. 1. Time–frequency windows used in (a) Fourier transform (FT), (b) a windowed Fourier transform (WFT), and (c) a wavelet transform (WT), and their corresponding time series represented in time space and frequency space.

components and an underrepresentation of the low-frequency components. Because of the constant frequency increment, the WFT does not have adequate resolution in the very low frequency band; much of the computation effort of the transfer is spent on high-frequency components, which results in a large number of spurious spectral peaks.

A WT uses generalized local base functions (wavelets) that can be stretched and translated with a flexible resolution in both frequency and time. The flexible windows are adaptive to the entire time–frequency domain, known as the wavelet domain (WD), which narrows while focusing on high-frequency signals and widens while searching the low-frequency background. Because of the “uncertainty principle” (cf. Chui 1992), the width and the height of a time–frequency window cannot be arbitrary. As a result, high precision in time localization in the high-frequency band can be achieved at the expense of reduced frequency resolution, and vice versa for low-frequency components (Fig. 1, right panel). In this way, a WT allows the wavelets to be scaled to match most of the high- and low-frequency signals so as to achieve the optimal resolution with the least number of base functions. This “zoom-in” property is a unique characteristic of WT that allows the localization of very short lived, high-frequency signals in time, such as abrupt changes, while resolving the low-frequency variability in the timescale or frequency more accurately with relative ease in computation.

Mathematically, a WT decomposes a signal $s(t)$ in terms of some elementary functions $\psi_{b,a}(t)$ derived from a “mother wavelet” or “analyzing wavelet” $\psi(t)$ by dilation and translation:

$$\psi_{b,a}(t) = \frac{1}{(a)^{1/2}} \psi\left(\frac{t-b}{a}\right), \quad (1)$$

where b denotes the position (translation) and $a(>0)$ the scale (dilation) of the wavelet; $\psi_{b,a}(t)$ are called “daughter wavelets” or, simply, “wavelets.” An energy normalization factor $(a)^{-1/2}$ in (1) keeps the energy of daughter wavelets the same as the energy of the mother wavelet. The wavelet transform of a real signal $s(t)$ with respect to the analyzing wavelet $\psi(t)$ may be defined as a convolution integral:

$$W(b,a) = \frac{1}{(a)^{1/2}} \int \psi^*\left(\frac{t-b}{a}\right) s(t) dt, \quad (2)$$

where ψ^* is the complex conjugate of ψ defined on the open “time and scale” real (b, a) half plane. The function $s(t)$ can be formally reconstructed from the wavelet coefficients by the inversion formula

$$s(t) = \frac{1}{C_\psi} \int \frac{da}{a^2} \int db \frac{1}{(a)^{1/2}} \psi\left(\frac{t-b}{a}\right) W_{b,a}, \quad (3)$$

where

$$C_\psi = \int_0^{+\infty} \frac{|\hat{\psi}(\omega)|^2}{\omega} d\omega < +\infty, \quad (4)$$

and $\hat{\psi}$ is the Fourier transform of ψ .

c. Graphical representation

An intuitive way to represent WT coefficients is similar to the way in which the musical tones are represented in a musical score.² Pioneers in the WT field have borrowed the concept of “octave,” which is logarithmic with the base of 2 for frequency or timescale, as a unit to divide the frequency domain. This unit allows us to include a broad range of scales, from very small to very large, in an efficient way in a coordinate system with linear interval in octave while logarithmic in frequency scale.

In a *continuous* WT where more scale decomposition is desired, each octave may be divided further by infinite voices. Practically, the voices are finitely chosen so that the scale ratio between any two consecutive voices in WD is fixed. For example, the scale ratio of two consecutive voices at any level i and $i+1$ of octave m is $a_{m,i}/a_{m,i+1} = \text{constant}$. The expression of a scale at octave m and voice i is $a_{m,i} = a_0 2^{m+i/v}$, where v is the number of voices per octave and a_0 is the scale at octave 0 and voice 0, which may be set at one’s disposal. In music, a_0 may be chosen to represent the timescale (proportional to the inverse of the frequency) at the middle C.

Thus, unlike the FT that maps a 1D time series to a 1D spectrum, the WT maps a 1D time series to a 2D image that portrays the evolution of scales and frequencies with time. Usually, the coefficients of a *continuous* WT are presented in the timescale $\{b, a\}$ half plane with linear scale on the time b axis, pointing to the right, and logarithmic scale a axis, facing downward with increasing scales in the octave (Fig. 2). To resolve localized signals, the analyzing wavelet $\psi(t)$ is chosen so that it vanishes outside some interval (t_{\min}, t_{\max}) . In this case, the domain in the $\{b, a\}$ half plane that can be influenced by a point (b_0, a_0)

mainly lies within the “cone of influence” defined by $|b - b_0| = a\Lambda$, where $\Lambda = 2^{1/2}$ for the Morlet wavelet we will use (see its expression in next section), with the vertex at the point (b_0, a_0) as shown in Fig. 2. The real part, the modulus and the phase of the $W(b, a)$, may be plotted separately in the same WD. The scale range is chosen depending on the frequency content of the timescales. For low-frequency (high frequency) variability a scale range containing only lower (higher) octaves is needed, similar to a bass (treble) clef in music. In general, a continuous scale covering both ends of the spectrum will be used. As a result, WT decomposes a signal into “localized” or “instantaneous” frequencies complete with the measure of intensity and duration for each frequency, analogous to the bass/treble clef, the crescendo/decrescendo, and the tempo in a piece of music. In other words, WT makes a time series sing!

d. Wavelet choice

There are many commonly used analyzing wavelets that can be grouped into two main categories: continuous wavelets and orthogonal wavelets. (A discrete wavelet transform may not be orthogonal.) One of the most widely used continuous wavelets in geophysics is the complex Morlet wavelet, which consists of a plane wave modified by a Gaussian envelope. Another commonly used continuous wavelet is the “Mexican hat,” which is the second derivative of the Gaussian function. The simplest orthogonal wavelet is the Haar wavelet, which is based on a box function. Other widely used orthogonal wavelets are the Daubechies wavelets with different orders that are compactly supported³ (Daubechies 1992). There are also semiorthogonal wavelets such as spline wavelets (Chui 1992). Descriptions of special properties of these wavelets can be found in the above-cited references and textbooks on wavelets. Here, we will not go into the pros and cons of using one wavelet over another. Suffice it to say that while a true physical signal should be independent of the choice of the wavelets, for best results, we need to use analyzing wavelets that bear reasonable resemblance in form to the signal. In general, orthogonal wavelets are desirable for use in decomposition and in reconstruction of time series with the minimal bases, as well as in solving partial differential equations (PDEs) (Perrier

²The range between a note at a C to the next higher or lower C, or from a G to the next higher or lower G, or so on, is called an “octave.” In fact, the frequency scale is constructed such that the frequency at, say, a C in one octave doubles that of the corresponding C in a lower octave while it halves the one in a higher octave. Thus, when we use “octave” as a unit to measure frequency, the frequencies of all C’s will be at a dyadic scale $2^m f_0$, where f_0 is the frequency of the middle C and $m (= 0, \pm 1, \pm 2, \dots)$ is an octave index. Higher (lower) octaves are indicated by positive (negative) octave index. In a well-tempered scale for western music, each octave contains 12 notes or “voices” that have specific frequencies.

³All continuous and some orthogonal wavelet bases consist of infinitely supported functions, although the influence at infinity is very small based on the wavelet’s definition. The orthogonal wavelets that satisfy the condition that the behavior of the signal at infinity does not play any role are *compactly supported*. In fact, the Haar wavelet is a degenerate case of Daubechies’ wavelets and is also a compactly supported wavelet.

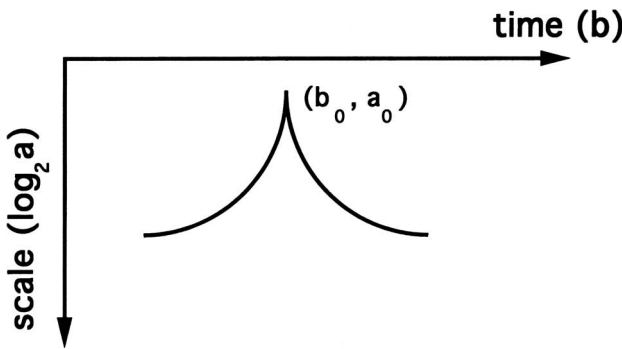


FIG. 2. Representation of wavelet transform in the real semiplane showing the scale (a ordinate, increasing downward) and translation (b abscissa) and the “cone of influence” at a point (b_0, a_0) .

1989; Liandrat et al. 1992). However, the orthogonal wavelets may not always yield the most physically meaningful scale analysis, because the scales are analyzed only at the *octaves* (integer powers of 2) not at the *voices* (fractional powers of 2). The redundancy of the continuous wavelets yields enhanced information on the timescale localization. However, due to the overcomplete bases, the information may not offer a perfect reconstruction. Thus, the orthogonal wavelets are better used for synthesis and data compression, while continuous wavelets are better used for scale analysis. In many ways, the aforementioned drawback in continuous wavelets may be reduced by selecting an appropriate discrete subset of continuous wavelet bases so that the subset would constitute a quasi-orthogonal frame, called a “wavelet frame.” On the other hand, the use of an appropriate interpolation may enable the computation of “continuous” wavelet coefficients from the orthogonal wavelet bases. The wavelet frame and the interpolation allow the user to combine the redundancy and the geometrical properties of the continuous WT with the economy of the orthogonal WT. Thus, in practice the distinction between the continuous WT and the orthogonal WT may not be so important, and depends more on the purpose of the application. In this paper, we deal with wavelike signals and therefore use the continuous Morlet wavelet (see Fig. 3) given by

$$\psi(t) = e^{ik_v t} e^{-|t|^2/2}. \quad (5)$$

The procedure for calculating the Morlet wavelet transform is the same as described in Weng and Lau (1994). One may use other continuous wavelets, such as the Mexican Hat. The advantage of using the Morlet wavelet is its complex nature that is able to detect both time-dependent amplitude and phase for different frequencies exhibited in the time series.

3. Analytic climate signal

One of the most important problems in the climate signal detection is the determination of trends in the presence of large climate variability. In the following, we illustrate the WT for four generic signals commonly encountered in the variability of the earth’s climate (Fig. 4):

- 1) Amplitude modulation:

$$s(t) = A(1 + \alpha \cos \Omega t) \cos \omega t; \quad (6)$$

- 2) Frequency modulation:

$$s(t) = B \cos(\omega t + m \sin \Omega t); \quad (7)$$

- 3) Abrupt change in frequency:

$$s(t) = \begin{cases} C \cos \omega_1 t & \text{for } t < 256, \\ C \cos \omega_2 t & \text{for } t \geq 256; \end{cases} \quad (8)$$

- 4) Abrupt change in time:

$$s(t) = D \frac{t - 256}{\sigma^2} \exp\left[-\frac{(t - 256)^2}{2\sigma^2}\right]. \quad (9)$$

The amplitude modulation signal (6) is often found in a climate system involving nonlinear interactions between different scales or interference of a frequency component from its sidebands. In the WD we define octave 0 as the period with 8 time units. Hence, octave 1 and octave 2 correspond to 16 and 32 time units, respectively, and so on. In this case each octave is divided by four voices. Equation (6) represents an oscillating signal with a fundamental period of 32 time

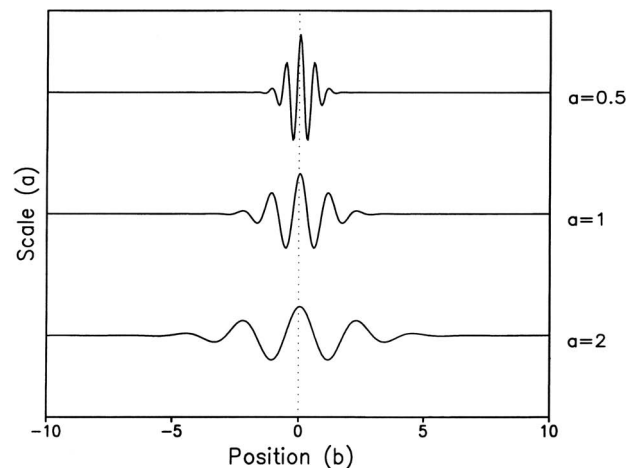


FIG. 3. Example of Morlet wavelet with different values of scale a , showing the different scales spanned by the influence cone.

units (octave 2), whose amplitude is modulated by a longer period of 256 time units. In the WD (lower panel of Fig. 4a), the dominant frequency appears as a horizontal line centered at octave 2, reflecting the constancy of the fundamental periodicity in time. The positive and negative phases of the waveform in the WT correspond to those in the original time series. The slight phase tilt in the waveform indicates the existence of sidebands of the primary frequency, as also seen in the corresponding FT power spectrum (Fig. 5a). The expansion of (6) represents the superposition of three frequencies ω and $\omega \pm \Omega$, in which constructive and destructive interference results in the amplitude modulation of ω by Ω .

The frequency modulation signal (7) may be important if the fundamental physical properties of the climate system undergo secular changes such as the increase in atmospheric moisture due to global warm-

ing. This may change the stability of the atmosphere and alter the frequency of its normal modes. The analytic signal (upper panel of Fig. 4b) is an oscillation with evolving fundamental frequencies that increase toward the center of the time domain ($t = 256$). In the WD (lower panel of Fig. 4b) this signal appears as oscillating elements forming an arch starting near octave 2 and decreasing to less than octave 0 at $t = 256$ and then returning to the original scale at $t = 512$. Since the frequencies are constantly evolving and any given single frequency does not exist for a finite time, the Fourier spectrum of this time series (Fig. 5b) shows no visibly dominant peaks and is indistinguishable from noise.

Another important climate signal is that associated with abrupt frequency change. This may be found in the occurrence of catastrophic event that has a long-term impact. Equation (8) shows an abrupt shift in

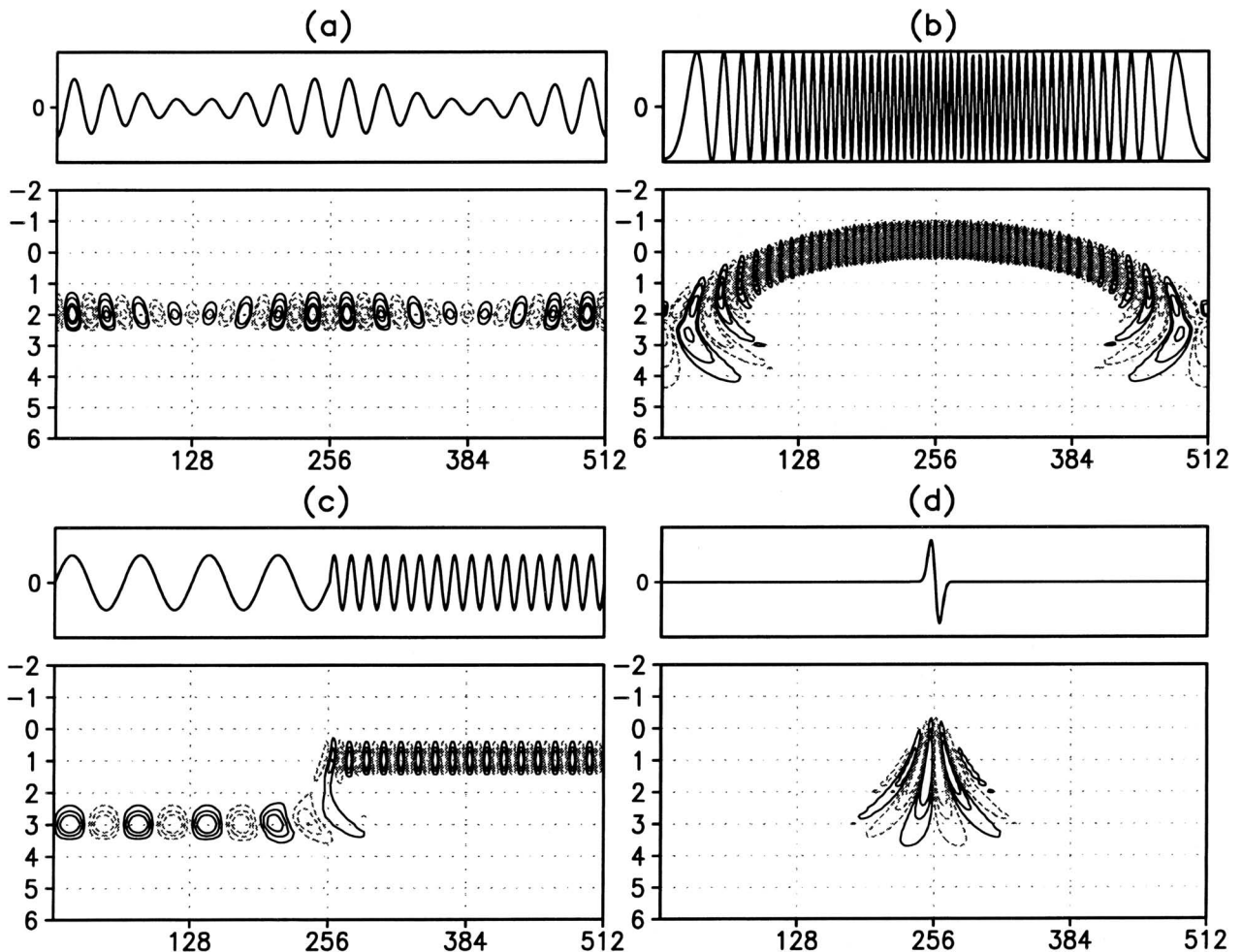


FIG. 4. Analytic signals and the real part of their Morlet wavelet transform in the time–frequency domain: (a) amplitude modulation, (b) frequency modulation, (c) abrupt change in frequency, and (d) abrupt change in time. The abscissa represents dimensionless time, and the ordinates are frequency in octaves in dyadic scales. Four voices are used in each octave. Octave 0 corresponds to a scale having 8 time units. The time series for each signal is shown in the top panel.

appearance of the oscillation near $t = 256$ in the original time series. In the WD (lower panel of Fig. 4c) this is represented by a shift in the scale from octave 3 to octave 1 at $t = 256$. The abruptness of the change is well represented by a few wavelets in the neighborhood of $t = 256$. The corresponding Fourier spectrum (Fig. 5c) shows two distinct peaks at the corresponding frequencies but contains no information on the time of occurrence of the abrupt change. Notice the presence of spurious spectral peaks near the fundamental frequencies. These peaks arise from the use of infinite base functions for finite sampling.

Finally, (9) represents a sudden finite-amplitude perturbation that is strongly damped and therefore has short-term but no long-term effects. In the earth's climate system, the effect of volcanic eruption on the global temperature variation may come under this category. The WD for this signal (lower panel of Fig. 4d) shows that the singular perturbation is well defined by convergence of the phase lines within the "cone of influence" centered at the time of occurrence of the perturbation at $t = 256$. As seen in the corresponding Fourier spectrum (Fig. 5d), a large number of components are needed to represent the signal. The time of occurrence and the exact form of the perturbation cannot be determined to the desired accuracy without using a large number of Fourier components (Fig. 5d).

4. Real climate time series

In this section, we present results of WT applied to two widely used climate time series. The first is a 2.5 million year (Myr) deep-sea sediment record of $\delta^{18}\text{O}$ at site 607 in the North Atlantic, which provides information on the variation of global ice volume (Raymo et al. 1990). This record is considered to be one of the longest proxy records for the earth's ancient climate. The second is the monthly Northern Hemisphere surface temperature (NHST) averaged from a 5×5 grid dataset for the period January 1854–July 1993. The NHST time series is one of few standard time series used by the International Panel for Climate Change in assessing of the impact of

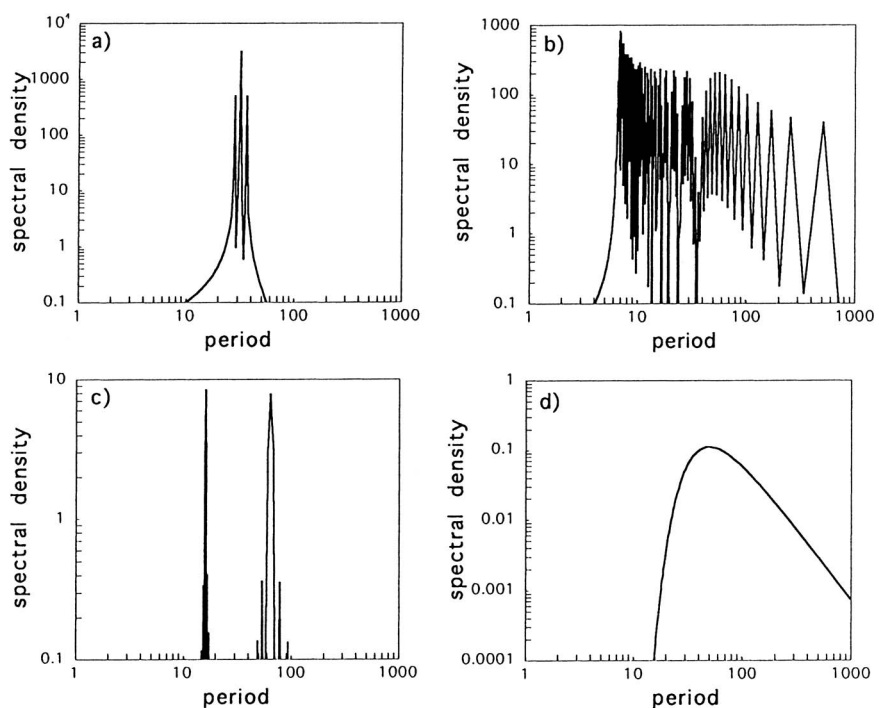


FIG. 5. Fourier spectra of the four time series presented in Fig. 4.

global change on contemporary climate. Both time series have been used extensively by climatologists to quantify the variability of the earth's ancient and contemporary climates.

a. Paleoclimate variability

The WT has been carried out with different scale resolutions and with different treatment of data at the end points to ensure stability of the frequency structures to be discussed. The WT for the $\delta^{18}\text{O}$ record (Fig. 6) shows that the global ice volume has two dominant regimes of quasi-periodic oscillations: 1) 40-kyr cycles for the period from 0.7 to 2.5 Myr and 2) 100-kyr cycles during the last 0.7 Myr, as indicated by the amplitude of the wavelet coefficients around octaves 2–3.5. In the sense of music, the WT unfolding of the $\delta^{18}\text{O}$ record is analogous to a melody that consists of two fundamental notes whose intensities vary with time. The WT shows clearly a steplike abrupt transition (compared to Fig. 4c) at around 0.7 Myr between the two frequency regimes. The shift in the frequency regime is clearly seen in the time mean wavelet spectrum (Fig. 7) for the two above regimes. (The time-mean spectra are obtained by averaging the WT coefficient over the corresponding time intervals.) For the past 2.5 Myr (Fig. 7a), the 40-kyr cycle dominates over the 100-kyr cycle. The dominance of the 100-kyr cycle during the past 0.7 Myr is quite apparent in the time mean spectra (Fig. 7b). In this spectrum where

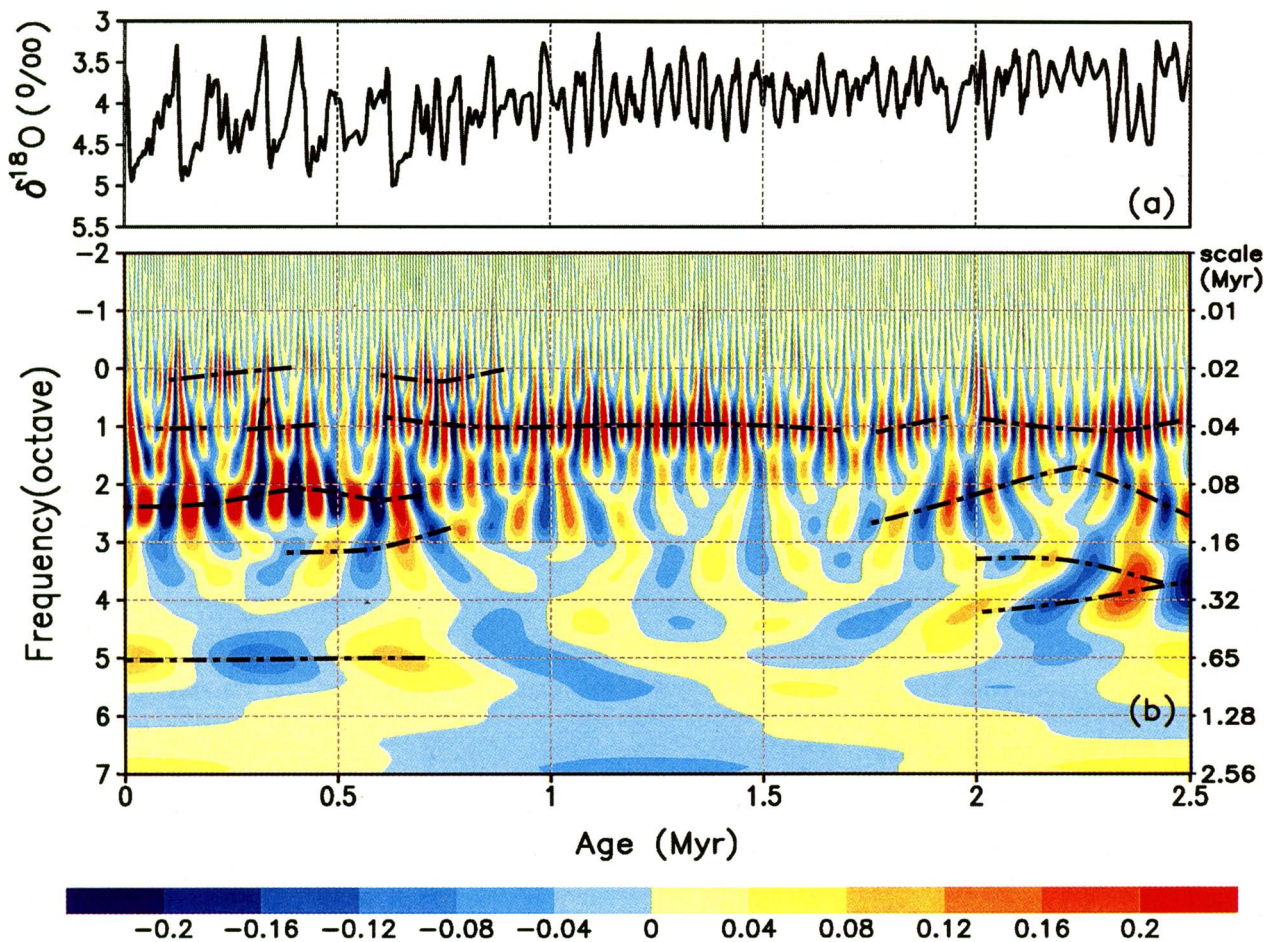


FIG. 6. (a) Time series for deep sea $\delta^{18}\text{O}$ at site 607 in the North Atlantic record for the past 2.5 Myr and (b) real part of its Morlet wavelet transform. Black dot-dashed lines in (b) indicate the frequency evolution of the dominant periodicities.

the 100-kyr cycle is predominant, the presence of the 640-kyr cycles and the quasi-20-kyr cycles, in addition to the 40-kyr cycle, are quite apparent, in contrast to the time period when the 40-kyr cycle is dominant (Fig. 7c). A closer examination of the WT in Fig. 6b and the modulus variation (not shown) reveals that the time history of the $\delta^{18}\text{O}$ record is characterized by frequency and amplitude modulation involving bifurcation and merging of dominant frequencies near the harmonics and subharmonics of the fundamental period $T \sim 40$ kyr—that is, 20, 80, 160 kyr, etc. Between 1.7 and 1 Myr, the 40-kyr cycle is most predominant, while the other subharmonics are relatively weak. At about 1.2 Myr, an abrupt bifurcation occurs with the revival of strong quasi-periodic cycles between 80 and 160 kyr and the appearance of a distinct 640-kyr cycle. In addition, there are noticeable enhancements of the oscillations at the period of about 20 kyr during the last 1 Myr when the 80–100-kyr cycles are strong. While the features of the dominant frequencies are consistent with previous

findings (e.g., Raymo et al. 1990), the WT yields a complete picture of time-frequency evolution that is impossible to achieve with the same accuracy by using WFT.

In addition, WT yields information on the trend in the data. Here, the trend in the data is represented by the longest resolvable cycle, at octave 8, that is, about 2.5 Myr. The WT (Fig. 6) indicates that the most rapid change of the trend occurs at about 1.2–1.0 Myr, where the 2.5-Myr cycle changes sign. This also coincides with the time when the frequency bifurcation and abrupt changes take place.

The two dominant cycles (40 and 100 kyr) coincide approximately with frequencies for two of the major components of orbital forcings associated with obliquity and eccentricity variations, while a less prominent periodicity (around 20 kyr) coincides with the cycle of precession of the equinoxes (Berger 1978). The WT results suggest that the frequency structure in the $\delta^{18}\text{O}$ record may be a reflection of nonlinear dynamical processes involving quasi-periodicity and/or

subharmonic mode locking under the influence of external forcings (Ecke 1991; Hilborn 1994). This provides an alternate view of the observed frequency structure in the evolution of the earth's paleoclimate and its relationship to orbital forcings (Liu 1992; Birchfield and Ghil 1993; and the references herein).

b. Contemporary climate variability

In this subsection, we turn to a WT description of the NHST anomaly for the period 1854–1993. The temperature time series and its real part of the Morlet wavelet coefficients are shown in Fig. 8. If the paleoclimate record in the previous section is likened to a simple melody, the NHST has the composition of a symphony. Three main frequency branches can be discerned: interannual (2–5 yr), interdecadal (10–12 yr, 20–25 yr, and 40–60 yr), and century (~180 yr) scales. During the early part of the record (before 1900), the decadal and bidecadal oscillations are quite strong, while the 2–5-yr cycles are sometimes very weak. During 1900–1940, a 5–6-yr oscillation becomes particularly pronounced, while the decadal

and bidecadal variabilities diminish and appear to merge toward an intermediate scale of approximately 16 yr. A most noticeable feature is the scale interaction across the interannual and interdecadal boundaries as indicated by the arch-shaped feature between 1900 and 1990, indicating the frequency modulation from a 5.6-yr cycle in the early 1900s to a quasi-10-yr cycle in the 1970s. Also emerging out of the 1900s is a 40–60-yr oscillation that is maintained up to the present. The century-scale variability indicated by a half-wave of 180-yr cycle represents the main trend in the NHST, with the most rapid increase around the 1920s. The above quasi-periodic cycles are punctuated by several singularities, indicated by the sharp converging WT phase lines onto the octave –1 axis, especially during the early part of the record (1854–1900). The strongest singularity is detected at the year 1893. Whether these represent short-term climatic events or glitches in the data record is impossible to determine without other independent data.

To provide a better qualitative description of the dominant frequency modes within each of the main frequency branches, Fig. 9 shows the time series of the wavelet coefficients for different frequency modes. The interannual variability includes two dominant frequencies around 2.4 and 4.8 yr. Separate calculations show that these two frequencies may be identified with those arising from the quasi-biennial oscillation (QBO) and the El Niño/Southern Oscillation (ENSO). The range in the interannual variability is relatively large (~0.2°C), compared to the total range (~0.5°C). The QBO variability is strong from 1870 to 1890 and from the mid-1960s to the mid-1980s but relatively weak from the 1900s to the 1950s, while the ENSO variability seems to have an inverse relationship to the QBO. This relationship is consistent with the merging and bifurcation of frequency regimes noted earlier. The interdecadal oscillations are strongly amplitude modulated, with the decadal oscillation most pronounced during the 1870s through the 1900s and from the 1960s to the 1980s and weakest during the 1910s through the 1950s (Fig. 9c). The bidecadal variations are strongest in the decades from the 1880s to the 1920s (Fig. 9d). The amplitude of the 40–60-yr cycle (represented by the 45-yr cycle in Fig. 9e) is on the rise since the beginning of the record. The average magnitude of the interdecadal variation is less than 0.1°C. Because of the endpoint effects, the phase of the interdecadal variability near the beginning and the end of the record may have less reliability.

Information concerning the trend in the NHST record, analyzed by WT, is mostly contained in the longest cycle at about 180 yr, as well as the 45-yr variability, while to a lesser extent in the 90-yr variability. The warming trend (see also the reconstruction in the

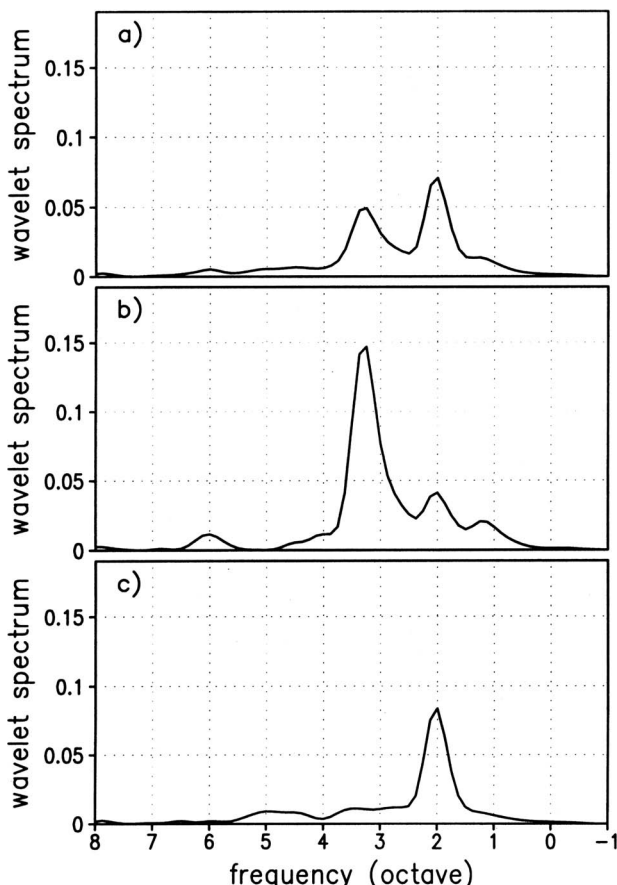


FIG. 7. Wavelet spectra for the $\delta^{18}\text{O}$ record averaged for the past (a) 2.5 Myr, (b) 0.7 Myr, and (c) 1–2.5 Myr. Octave 0 corresponds to the timescale of 10 kyr.

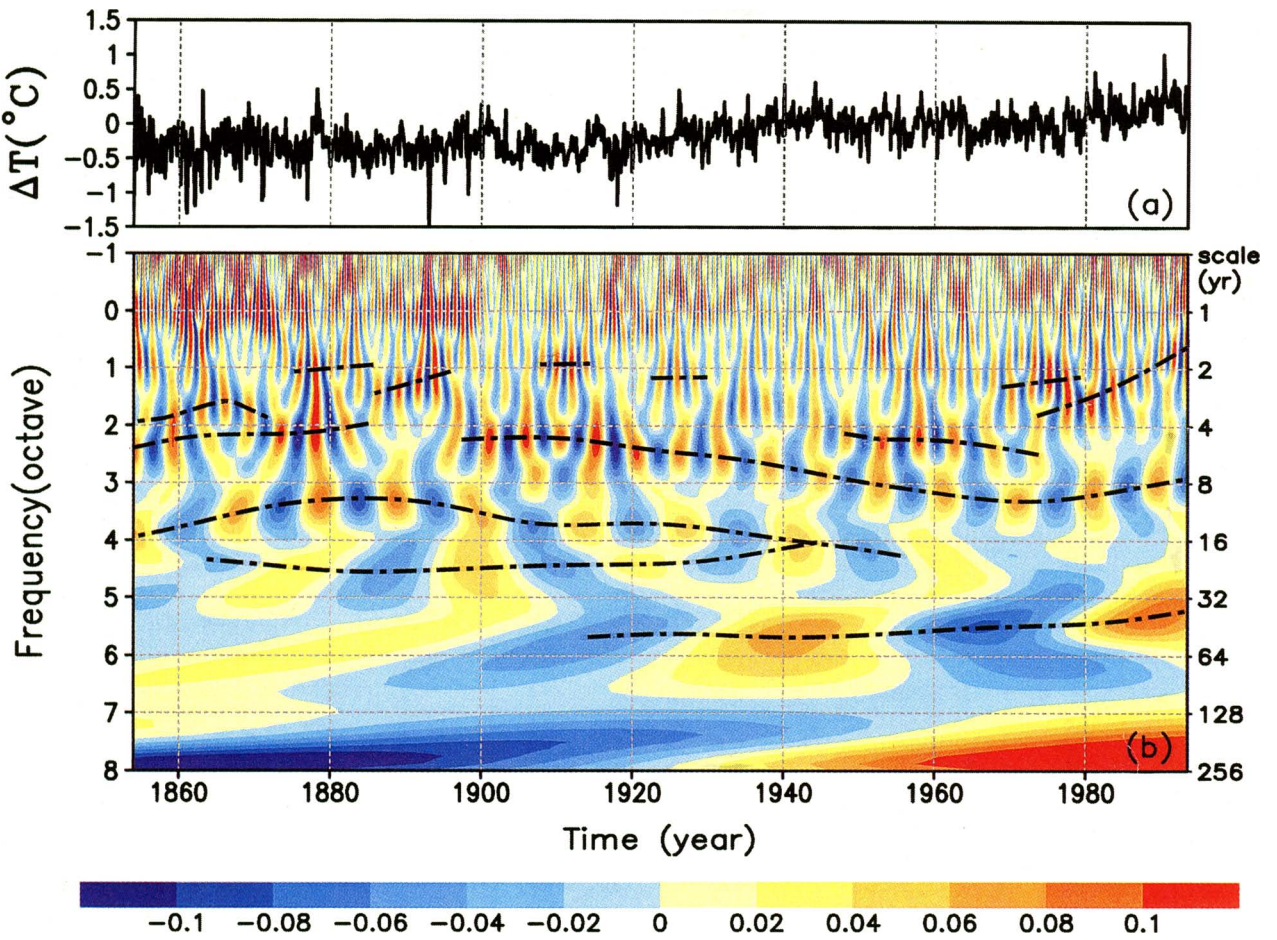


FIG. 8. (a) The time series of the Northern Hemisphere surface temperature and (b) the real part of its Morlet wavelet coefficients. Black dot-dashed lines in (b) indicate the frequency evolution of the dominant periodicities.

bottom panel of Fig. 9) is captured by the upward swing of the 180-yr cycle during the 1920s, with most of the warming occurring during the last 20 yr. This feature has been noted in many previous studies of the same data but with a different methodology (e.g., Jones et al. 1986). The warm periods in the 1940s and 1980s are also due to the warm phase of the 45-yr oscillation; the latter, along with the warmest phase in the 180-yr variability, may contribute to the record warm global temperature in 1988 and 1990 (cf. Kerr 1991). The warming period from the 1960s to the early 1990s appears to usher in a new climatic regime with enhanced QBO but reduced ENSO cycles (Fig. 9a).

For the NHST, the relevant external forcings are the annual and semiannual cycles, and possibly the solar cycles associated with the decadal and secular cycles (Friis-Christensen and Lassen 1991). The presence of WT peaks at the above periodicities and at their near subharmonics is consistent with the notion that the NHST represents competing influences of internal oscillation mechanisms and nonlin-

ear frequency entrainment or phase locking by solar forcings at fixed periodicities.

c. Further discussion

The results for the NHST may also be relevant to a recent debate on the physical existence of the interdecadal oscillations in the global surface air temperature record. The presence of a bidecadal and a 65–70-yr oscillation in the global temperature fluctuation have been reported, respectively, by Ghil and Vautard (1991) and Schlesinger and Ramankutty (1994) using singular spectrum analysis (SSA). However, Elsner and Tsonis (1991) pointed out that the presence of bidecadal oscillation may be questionable because the detection of these oscillations are dependent upon whether the early part of the data is included in the analysis. Elsner and Tsonis (1994) also pointed out that the statistics of the 65–70-yr cycles in the data may not be distinguishable from red noise.

The discrepancy regarding the bidecadal oscillation in the global surface temperature may be under-

standable based on our WT results of NHST. The WT results (Fig. 8) show that the amplitudes of the bidecadal cycles are strongest before the 1990s, while those for the 5–6-yr oscillations are relatively weak. After the 1900s, the 5–6-yr cycles are much stronger and the bidecadal variability diminishes in amplitude while shifting toward higher frequencies. Because of the nonstationary nature of the oscillation, any analysis that involves temporal averaging using a fixed-width window, such as SSA, may result in a smearing of the amplitude of the interannual and interdecadal bands. Depending on which subsets of the record are used, reordering the dominant EOF or even dropping the otherwise “significant” EOFs below the noise floor may occur. Because WT bases are localized, the transform does not suffer from the averaging process inherent in all EOF-based techniques.

At present, one of the shortcomings of the WT analysis is the lack of a proper statistical significance test for nonstationary processes, in general, and for WT, in particular. Almost all traditional significance tests are derived from the assumption of identical repeated cycles for nonstationary processes and therefore are inappropriate for WT. An alternative is to use Monte Carlo methods. However, Monte Carlo methods are also unsatisfactory in the context of nonlinear systems, whereby one is seeking for localization of frequencies that may be a part of a hierarchy of frequency structures related to the fundamental driving frequencies. Some of the higher harmonics have small amplitudes and may be difficult to distinguish from noise. Yet their presence in conjunction with the fundamental frequencies is physically important but not necessarily statistically significant in the traditional sense. In this regard, the results of the WT analysis including the bidecadal variations and the 40–60-yr cycles can be considered only tentative and have to be validated awaiting a proper statistical significance test and physical considerations. The formulation of a proper statistical significance test for WT is an important research topic in its own right and is beyond the scope of this paper.

Despite these caveats, the results from the WT analysis of the above-mentioned two independent climate time series with widely different timescales have revealed a possible *universal* interpretation of the earth’s climate. Periodic forcings external to the earth’s climate system may provide *attracting* frequencies—that is, subharmonics of the forcing frequencies—for localization of the observed frequencies of the climate system. It is plausible that the earth’s climate may be entrained into or mode locked to one or more of these attracting frequencies over a wide range of parameters (Alifov and Frolov 1990; Tsonis 1992). The frequency entrainment does not

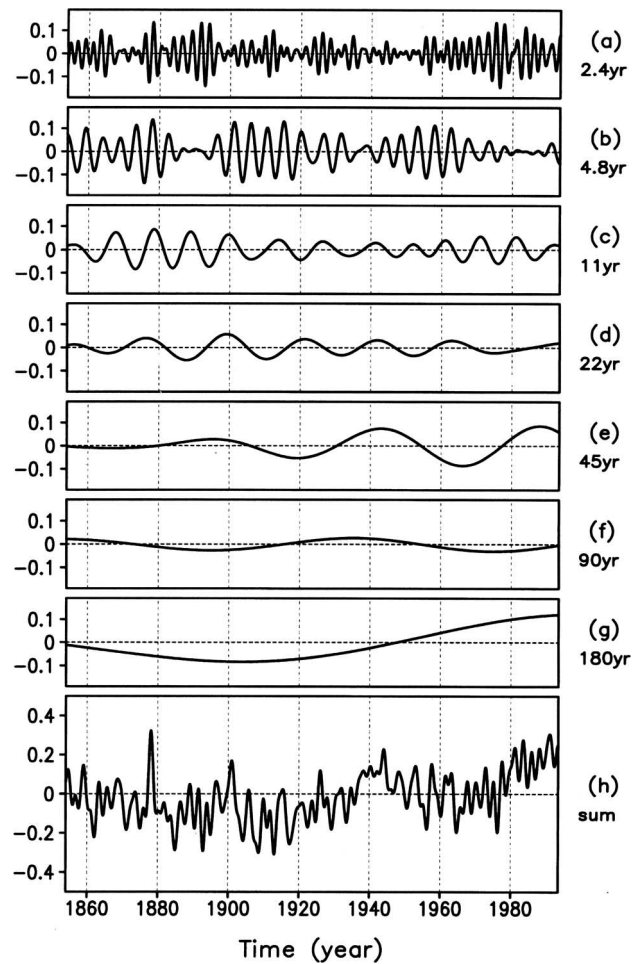


FIG. 9. Time variation of NHST anomalies due to the dominant cycles for the interannual band (2.4 and 4.8 yr), the decadal to interdecadal bands (11, 22, and 45 yr), and the century to intercentury bands (90 and 180 yr). The last panel shows the reconstruction of the original NHST time series using all the above periodicities. The unit of the ordinate in all panels is $^{\circ}\text{C}$.

require a large amount of energy at the attracting frequency but instead depends upon the strength of nonlinear coupling within the system. This may provide an explanation as to why climate signals are often found with periodicities near the solar cycles or earth orbital and rotational cycles and near their harmonics and subharmonics—that is, the 20-, 40-, and 100-kyr orbital forcings for the $\delta^{18}\text{O}$ time series and the solar cycles at 11 and 22 yr for the NHST time series—despite the small fraction of solar energy present at these frequencies.

5. Concluding remarks

In this paper, we have provided an introduction and a tutorial for using WT for climate time series analysis,

using examples from analytic signals and from real climate time series. The analogy between WT representation of a time series and music provides an understanding of the importance of local versus global information in the time-frequency localization of climate signals. We find that the time-frequency information provided by WT is comprehensive and unmatched by FT or windowed FT. Results of the WT for two popular climate time series have also provided a new perspective on the nonlinear dynamical underpinnings of the variations of the earth's climate under external forcings. We hope these results will inspire further use of WT for climate analysis.

Acknowledgments. The authors wish to thank Prof. Hartmann for providing the $\delta^{18}\text{O}$ time series, and Prof. A. Robock and Mr. J. Mao for providing the Jones et al. Northern Hemisphere surface temperature data for the wavelet analysis. Thanks also go to Laura Rumburg for her professional draft of Fig. 1. Prof. A. Tsonis provided constructive criticism and brought our attention to recent publications that are directly relevant to the results presented in this paper. This work was partially supported by NASA, Modeling and Data Analysis Program and the Earth Observing System/Interdisciplinary Investigation, Office of Mission to Planet Earth. Part of the work was done when HW was supported by the National Research Council's Research Associateship Program.

References

- Alifov, A. A., and K. V. Frolov, 1990: *Interaction of Nonlinear Oscillatory Systems with Energy Sources*. Hemisphere Publishing Co., 327 pp.
- Berger, A., 1978: Long-term variations of caloric insolation resulting from the earth's orbital elements. *Quat. Res.*, **9**, 139–167.
- Birchfield, G. E., and M. Ghil, 1993: Climate evolution in the Pliocene and Pleistocene from marine-sediment records and simulations: Internal variability versus orbital forcing. *J. Geophys. Res.*, **98**, 10 385–10 399.
- Chui, C. K., 1992: *An Introduction to Wavelets*. Academic Press, Inc., Harcourt Brace Jovanovich, 266 pp.
- Collineau, S., and Y. Brunet, 1993: Detection of turbulent coherent motions in a forest canopy. Part I: Wavelet analysis. *Bound.-Layer Meteor.*, **65**, 357–379.
- Combes, J. M., A. Grossmann, and Ph. Tchamitchian, 1989: Wavelets: Time-frequency methods and phase space. *Proc. Int. Conf.*, Marseille, France, 331 pp.
- Daubechies, I., 1992: *Ten Lectures on Wavelets*. Society for Industrial and Applied Mathematics, 357 pp.
- Ecke, R. E., 1991: Quasiperiodicity, mode-locking, and universal scaling in Rayleigh-Bénard convection. *Chaos, Order, and Patterns*, R. Artuso, P. Cvitanović, and G. Casatić, Eds., Plenum Press, 77–108.
- Elsner, J. B., and A. A. Tsonis, 1991: Do bidecadal oscillations exist in the global temperature record? *Nature*, **353**, 551–553.
- , and —, 1994: Low-frequency oscillation. *Nature*, **372**, 507–508.
- Farge, M., 1992: Wavelet transforms and their applications to turbulence. *Ann. Rev. Fluid Mech.*, **24**, 395–457.
- Friis-Christensen, E., and K. Lassen, 1991: Length of the solar cycle: An indicator of solar activity closely associated with climate. *Science*, **254**, 698–700.
- Gabor, D., 1946: Theory of communications. *J. IEEE (London)*, **93**, 429–457.
- Gamage, N., and W. Blumen, 1993: Comparative analysis of low-level cold fronts: Wavelet, Fourier, and empirical orthogonal function decompositions. *Mon. Wea. Rev.*, **121**, 2867–2878.
- Gambis, D., 1992: Wavelet transform analysis of the length of the day and the El Niño/Southern Oscillation variations at intraseasonal and interannual time scales. *Ann. Geophys.*, **10**, 429–437.
- Gao, W., and B. L. Li, 1993: Wavelet analysis of coherent structures at the atmosphere–forest interface. *J. Appl. Meteor.*, **32**, 1717–1725.
- Ghil, M., and R. Vautard, 1991: Interdecadal oscillations and the warming trend in global temperature time series. *Nature*, **350**, 324–327.
- Gollmer, S., Harshvardhan, R. F. Cahalan, and J. B. Snider, 1995: Windowed and wavelet analysis of marine stratocumulus cloud inhomogeneity. *J. Atmos. Sci.*, **52**, 3013–3030.
- Hilborn, R. C., 1994: *Chaos and Nonlinear Dynamics; An Introduction for Scientists and Engineers*. Oxford University Press, 654 pp.
- Jones, P. D., S. C. B. Raper, R. S. Bradley, H. F. Diaz, P. M. Kelly, and T. M. L. Wigley, 1986: Northern Hemisphere surface air temperature variations: 1851–1984. *J. Climate Appl. Meteor.*, **25**, 161–179.
- Kerr, R. A., 1991: Global temperature hits record again. *Science*, **251**, 274.
- Kumar, P., and E. Foufoula-Georgiou, 1993: A new look at rainfall fluctuations and scaling properties of spatial rainfall using orthogonal wavelets. *J. Appl. Meteor.*, **32**, 209–222.
- Liandrat, J., V. Perrier, and Ph. Tchamitchian, 1992: Numerical resolution of nonlinear partial differential equations using the wavelet approach. *Wavelets And Their Applications*, M. B. Ruskai et al., Eds., Jones and Bartlett Publishers, 227–238.
- Liu, H., 1992: Frequency variations of the Earth's obliquity and the 100-kyr ice-age cycles. *Nature*, **358**, 397–399.
- Meyers, S. D., B. G. Kelly, and J. J. O'Brien, 1993: An introduction to wavelet analysis in oceanography and meteorology: With application to the dispersion of Yanai waves. *Mon. Wea. Rev.*, **121**, 2858–2866.
- Morlet, J., 1983: Sampling theory and wave propagation. *NATO ASI Series*, Fl, Springer, 233–261.
- Perrier, V., 1989: Towards a method for solving partial differential equations using wavelet bases. *Wavelets*, Combes et al., Eds., Springer-Verlag, 269–283.
- Raymo, M. E., W. F. Ruddiman, N. J. Shackleton, and D. W. Oppo, 1990: Evolution of Atlantic–Pacific $\delta^{13}\text{C}$ gradients over the last 2.5 m.y. *Earth Planet. Sci. Lett.*, **97**, 353–368.
- Ruskai, M. B., G. Beylkin, R. Coifman, I. Daubechies, S. Mallat, Y. Meyer, and L. Raphael, Eds., 1992: *Wavelets and Their Applications*, Jones and Bartlett, 474 pp.
- Schlesinger, M. E., and N. Ramankutty, 1994: An oscillation in the global climate system of period 65–70 years. *Nature*, **367**, 723–726.
- Tsonis, A. A., 1992: *Chaos: From Theory to Applications*. Premium Press, 274 pp.
- Weng, H.-Y., and K.-M. Lau, 1994: Wavelet, period-doubling and time-frequency localization with application to satellite data analysis. *J. Atmos. Sci.*, **51**, 2523–2541.